ЖУРНАЛ СТРУКТУРНОЙ ХИМИИ

*2017. Том 58, № 1* *Январь – февраль* *С. 174 – 179*

*КРАТКИЕ СООБЩЕНИЯ*

UDC 548.737

# SOLVENT EFFECTS ON THE NH STRETCHING OF 1-(4-PYRIDYL)PIPERAZINE

**C. Parlak**

*Department of Physics, Science Faculty, Ege University, Izmir, Turkey*
E-mail: cparlak20@gmail.com

*Received November, 18, 2015*

The solvent effects on the NH stretching of 1-(4-pyridyl)piperazine (1-4pypp, $C_9H_{13}N_3$) are investigated by density functional theory (DFT). The B3LYP hybrid density functional is used with the 6-311+G(3*df*,*p*) basis set in the polarizable continuum model (PCM). Computations are performed with 18 different polar or non-polar solvents. The calculated frequencies of the solvent-induced NH stretching vibrations are correlated with some solvent parameters such as the Kirkwood—Bauer—Magat (KBM) equation, the solvent acceptor number (*AN*), Swain parameters, and the linear solvation energy relationships (LSER). The present work explores the effects of the medium on the ν(NH) vibrations. The findings of this research can be useful for piperazines.

DOI: 10.15372/JSC20170122

**Keywords:** 1-(4-pyridyl)piperazine, DFT, NH stretching, solvent effect.

Piperazines exhibit a wide range of pharmacological activities such as antibacterial, antifungal, antitubercular, anticancer, antiviral, and antioxidant [ 1 ]. One of piperazine derivatives, 1-(4-pyridyl)piperazine or 1-(pyrid-4-yl)piperazine, is a versatile molecule. It has been mainly used as a pharmaceutical intermediate. For instance, 1-4pypp has been employed in the chemical structure of some drugs used for treatment of hypertension [ 2 ], HIV-1 [ 3 ], nephritis [ 4 ].

Solvent effects on vibrational frequencies and intensities have been well known [ 5—8 ]. The characteristic infrared stretching vibrations of solute structures have been extensively studied. There are numerous works on the solvent effect on frequencies of some groups [ 7—13 ]. Moreover, several empirical approaches attempt to characterize the solvent effects on vibrational frequencies, such as KBM [ 14, 15 ], *AN* [ 16 ], Swain [ 17 ], and LSER [ 18 ] equations. We also reported the solvent effects on the vibrational frequencies of some organic compounds [ 19—21 ].

In 2010, Alver and Şenyel examined the vibrational spectra and conformations for the powder form of 1-4pypp [ 22 ]. DFT data showed that the equatorial-equatorial (e-e) conformer is the most stable form of the compound. In another study conducted by Mary and coworkers in 2014 [ 23 ], the acid-base properties, vibrational spectra, NBO analysis for the single crystal form of the compound were also studied both experimentally and theoretically. The conformational preference (e-e) is in agreement with the results obtained from the XRD data [ 23 ]. In continuation of our interests in the investigation of solvent effects on the vibrational frequencies [ 19—21, 24 ], the prime objective of the present study was to use DFT in conjunction with the B3LYP/6-311+G(3*df*,*p*) method to examine the solvent effects on the NH stretching of 1-4pypp. Further, the frequencies of NH stretching vibrations were correlated with the KBM, *AN*, Swain, and LSER solvent scales.

**Computational methodology.** All the computations were carried out by a cluster system with a pre-compiled set of the Gaussian 09 program [ 25 ], configured for parallel computing. All structural

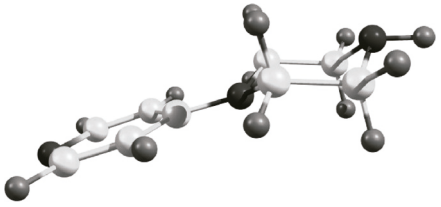

*Fig. 1.* Optimized structure for the e-e conformer of 1-4pypp

illustrations were made with the GaussView 5.0.8 program [ 26 ]. For all the computations, the e-e conformer of 1-4pypp in various solvents (Fig. 1) were optimized using the B3LYP functional in conjunction with the 6-311+G(3*df*,*p*) basis set. 18 different solvents were employed to investigate the solute-solvent interactions. PCM was used to study the solvent effects [ 27 ]. Harmonic vibrational frequencies, scaled by 0.9683 [ 28 ], were also computed with the same functional and basis set.

The KBM equation is given as follows:

$$\frac{\nu_0 - \nu_s}{\nu_0} = A\frac{\varepsilon - 1}{2\varepsilon + 1} = A\,f(\varepsilon),$$

where $\nu_0$ and $\nu_s$ are the vibrational frequencies of the solute in the gas phase and the solvent, respectively, $\varepsilon$ is the dielectric constant of the solvent, while $A$ is a constant depending on the dimensions and electrical properties of the vibrating solute dipole [ 14, 15 ]. The equation can be changed to the general form as $\nu_s = \nu_0 - C(\varepsilon - 1)/(2\varepsilon + 1)$, where $C$ equals $A\nu_0$. When the correlation between $\nu_s$ and $f(\varepsilon)$ is linear, the slope is $C$ and $\nu_0$ is the intercept.

The equation of the solvent *AN* is given as

$$\nu = \nu_0 + K\,AN.$$

Here, $\nu_0$ is the vibrational frequency of a solute in hexane and $K$ is the sensitivity of the vibrational frequency ($\nu$) to the solvent *AN* [ 16 ].

The equation of the Swain model is given by

$$\nu = \nu_0 + aA_j + bB_j$$

$\nu$ is the vibrational frequency of a solute in presence of a solvent. $\nu_0$ represents the predicated value of *n*-heptane as a reference solvent. $A_j$ and $B_j$ are measures of the solvent hydrogen-bond donor (HBD) acidity and the solvent hydrogen-bond acceptor (HBA) basicity, correspondingly. a and b represent the sensitivity of solute to a solvent change [ 17 ].

The equation of LSER model is given as follows:

$$\nu = \nu_0 + (s\pi^* + d\delta) + a\alpha + b\beta$$

where $\nu$ is the vibrational frequency of a solute in a solvent, $\nu_0$ is the regression value of $\nu$ in cyclohexane as a reference solvent, $\pi^*$ is an index of solvent dipolarity/polarizability, $\delta$ is a discontinuous polarizability correction term for polychlorinated aliphatic hydrocarbon and aromatic solvents. $\alpha$ and $\beta$ are the measures of the solvent HBD acidity and HBA basicity, respectively. The regression coefficients *s*, *d*, *a*, and *b* can provide quantitative measures of the relative contribution of the indicated parameters [ 18 ]. The KBM, *AN*, Swain, and LSER parameters of the solvents used in the present study are presented in Table 1 [ 29, 30 ].

**Results and discussion.** Free energy, dipole moment, NH bond length, and stretching frequency for the optimized geometries of the e-e conformer of 1-4pypp in solutions are listed in Table 2. Solvent-induced unscaled NH frequency vs. energy plot for the compound is depicted in Fig. 2, *a*. The e-e conformer of the compound is stabilized as the polarity of the solvents increases. There is a linear correlation between the frequency and energy values ($R^2$ = 0.99980 and 0.99981 for unscaled and scaled frequencies, respectively). The relationships between the NH bond lengths and unscaled stretching frequencies are shown in Fig. 2, *b*. It was noticed that the NH bond lengths showed good and linear correlations with the $\nu$(NH) frequencies ($R^2$ = 0.99924 and 0.99926 for unscaled and scaled frequencies, respectively). These NH bond lengths increase with a decrease in the $\nu$(NH) frequencies and an increase in the solvent polarity. Plot of the dipole moment vs. $\nu$(NH) vibration is also shown in Fig. 2, *c*. There are also good and linear correlations between the NH frequencies and dipole moments ($R^2$ = 0.99784 and 0.99790 for unscaled and scaled frequencies, respectively). The dipole moment in-

Table 1

*Solvent parameters*

| Solvent | $f(\varepsilon)$ | *AN* | π* | δ | α | β | $A_j$ | $B_j$ |
|---|---|---|---|---|---|---|---|---|
| *n*-hexane | 0.186 | 0.0 | –0.04 | 0.0 | 0.00 | 0.00 | 0.01 | –0.01 |
| Cyclohexane | 0.203 | 1.6 | 0.00 | 0.0 | 0.00 | 0.00 | 0.02 | 0.06 |
| Diethylether | 0.345 | 3.9 | 0.27 | 0.0 | 0.00 | 0.47 | 0.12 | 0.34 |
| Toluene | 0.245 | 6.8 | 0.54 | 1.0 | 0.00 | 0.11 | 0.13 | 0.54 |
| Tetrahydrofuran | 0.405 | 8.0 | 0.58 | 0.0 | 0.00 | 0.55 | 0.17 | 0.67 |
| Benzene | 0.231 | 8.2 | 0.59 | 1.0 | 0.00 | 0.10 | 0.15 | 0.59 |
| Tetrachloromethane | 0.226 | 8.6 | 0.28 | 0.5 | 0.00 | 0.10 | 0.09 | 0.34 |
| 1,4-dioxane | 0.223 | 10.8 | 0.55 | 0.0 | 0.00 | 0.37 | 0.19 | 0.67 |
| Acetonitrile | 0.479 | 18.9 | 0.75 | 0.0 | 0.19 | 0.40 | 0.37 | 0.86 |
| Dichloromethane | 0.422 | 20.4 | 0.82 | 0.5 | 0.13 | 0.10 | 0.33 | 0.80 |
| Chloroform | 0.359 | 23.1 | 0.58 | 0.5 | 0.20 | 0.10 | 0.42 | 0.73 |
| 2-Butanol | 0.454 | 32.0 | 0.40 | 0.0 | 0.69 | 0.80 | — | — |
| 2-Propanol | 0.460 | 33.6 | 0.48 | 0.0 | 0.76 | 0.84 | 0.59 | 0.44 |
| Ethanol | 0.471 | 37.9 | 0.54 | 0.0 | 0.86 | 0.75 | 0.66 | 0.45 |
| Methanol | 0.478 | 41.5 | 0.60 | 0.0 | 0.98 | 0.66 | 0.75 | 0.50 |
| Acetone | 0.465 | 12.5 | 0.62 | 0.0 | 0.08 | 0.48 | 0.25 | 0.81 |
| *n*-heptane | 0.190 | 0.0 | 0.00 | 0.0 | 0.00 | 0.00 | 0.00 | 0.00 |
| Dimethylsulfoxide | 0.484 | 19.3 | 0.76 | 0.0 | 1.00 | 0.00 | 0.34 | 1.08 |

Table 2

ν(NH) *frequencies and some parameters of* 1-4pypp

| Solvent | Dipole Moment, Debye | NH Bond Length, Å | Unscaled ν(NH), $cm^{-1}$ | Scaled ν(NH), $cm^{-1}$ | Free Energy, Hartree |
|---|---|---|---|---|---|
| *n*-Hexane | 5.51 | 1.01 | 3533 | 3421 | –515.016 |
| Cyclohexane | 5.52 | 1.01 | 3533 | 3421 | –515.016 |
| Diethylether | 5.57 | 1.01 | 3533 | 3421 | –515.016 |
| Toluene | 5.64 | 1.01 | 3532 | 3421 | –515.016 |
| Tetrahydrofuran | 5.65 | 1.01 | 3532 | 3420 | –515.016 |
| Benzene | 5.66 | 1.01 | 3532 | 3420 | –515.016 |
| Tetrachloromethane | 5.69 | 1.01 | 3532 | 3420 | –515.017 |
| 1,4-dioxane | 6.06 | 1.01 | 3530 | 3418 | –515.019 |
| Acetonitrile | 6.12 | 1.01 | 3530 | 3418 | –515.019 |
| Dichloromethane | 6.31 | 1.01 | 3529 | 3417 | –515.020 |
| Chloroform | 6.36 | 1.01 | 3528 | 3416 | –515.020 |
| 2-Butanol | 6.50 | 1.01 | 3527 | 3416 | –515.021 |
| 2-Propanol | 6.53 | 1.01 | 3527 | 3415 | –515.022 |
| Ethanol | 6.54 | 1.01 | 3527 | 3415 | –515.022 |
| Methanol | 6.56 | 1.01 | 3527 | 3415 | –515.022 |
| Acetone | 6.59 | 1.01 | 3527 | 3415 | –515.022 |
| *n*-heptane | 6.60 | 1.01 | 3527 | 3415 | –515.022 |
| Dimethylsulfoxide | 6.62 | 1.01 | 3527 | 3415 | –515.022 |

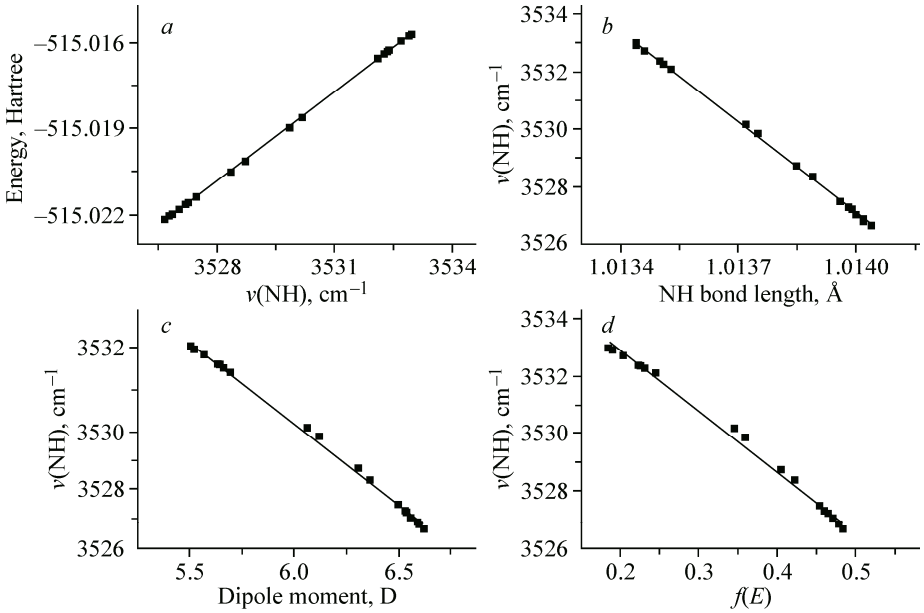


*Fig. 2.* Plot of the NH frequency vs. the optimized energy (*a*), NH bond length (*b*), dipole moment (*c*), and KBM parameter (*d*) of 1-4pypp

creases gradually from lower to higher dielectric and it is in agreement with the literature data [ 19, 20 ]. It also increases with a decrease in the ν(NH) frequencies.

Turning to the vibrational frequencies, the ν(NH) bands of powder 1-4pypp were observed at 3241 $cm^{-1}$ and 3248 $cm^{-1}$ in the IR and Raman spectra [ 22 ], whereas these bands of its crystal form were observed at 3383 $cm^{-1}$, 3223 $cm^{-1}$, and 3245 $cm^{-1}$ in the IR and Raman spectra [ 23 ], respectively. The splitting is due to the Davydov coupling between the neighboring units [ 23 ]. Furthermore, in the gas phase, this band was computed by B3LYP/6-31G(*d*) to be at 3345 $cm^{-1}$ (dual scaling) [ 22 ] while it was calculated by HF, B3PW91, and B3LYP with the 6-31G(*d*) basis set to be at 3368 $cm^{-1}$, 3453 $cm^{-1}$, and 3367 $cm^{-1}$ (uniform scaling) [ 23 ], respectively. In the present study, the NH stretching frequencies computed at the B3LYP/6-311+G(3*df*,*p*) level for 1-4pypp in solutions are listed in Table 3. For *n*-hexane, the NH vibrations are computed at higher frequencies. This belongs to the free monomer state of NH since no remarkable solute-solvent interactions occur in inert solvent *n*-hexane. Interestingly, the NH band was found at lower frequencies in polar solvents.

Fig. 2, *d* demonstrates the NH frequency vs. the parameter of the KBM equation. As seen from Table 3 and Fig. 2, *d*, there is a linear correlation between ν(NH) and $f(\varepsilon)$. The negative slope indi-

Table 3

KBM, *AN*, Swain, *and* LSER *equations for the solvent-induced* ν(NH) *vibrations*

| Frequency | Model | Equation | $R^2$ |
|---|---|---|---|
| Unscaled | KBM | $3537.13 - 21.25f(\varepsilon)$ | 0.99478 |
| | LSER | $3532.88 - 5.62\pi^* + 2.37\delta - 2.11\alpha - 1.58\beta$ | 0.87340 |
| | Swain | $3533.38 - 7.18A_j - 3.16B_j$ | 0.76142 |
| | *AN* | $3532.06 - 0.15AN$ | 0.61039 |
| Scaled | KBM | $3425.00 - 20.58f(\varepsilon)$ | 0.99488 |
| | LSER | $3420.89 - 5.45\pi^* + 2.30\delta - 2.04\alpha - 1.53\beta$ | 0.87357 |
| | Swain | $3421.37 - 6.95A_j - 3.06B_j$ | 0.76173 |
| | *AN* | $3420.09 - 0.15AN$ | 0.61055 |

cates that these frequencies are red-shifted with an increase in the dielectric constant of the solvent employed. Although the specific and the non-specific solvent effects contribute to solute-solvent interactions, KBM only considers the solvent dielectric constants. Also, the vibrational frequencies depend on the dielectric constant of the solvent. These facts evidence a good relationship between the KBM parameter and the ν(NH) frequency. The results confirm that the PCM model is suitable to predict the dielectric-induced solvent effect on the vibrational frequency. Similar studies were reported for the KBM equation with both theoretical [ 13, 24, 31 ] and experimental data [ 8 ]. The *AN* equations are also listed in Table 3. There is a poor correlation between ν(NH) and *AN*. These results show that the *AN* equation does not play a major role in the determination of vibrational shifts in solutions.

According to Swain, there are two types of the solvent effect [ 17 ]. They are the anion-solvating tendency of the solvent (acidity) and the cation-solvating tendency of the solvent (basicity). This implies that only the specific solute-solvent interactions are considered. Although the correlations of the Swain equation for ν(NH) are poor, they are better than those noticed with *AN* (Table 3). It is probable that both Lewis acidity and basicity for the solvent are considered in the Swain equation whereas *AN* considers only the Lewis acidity of the solvent. The negative signs for $A_j$ and $B_j$ represent that the solvent HBD acidity and HBA basicity lead to a red shift of ν(NH). The ratios of these coefficients are almost 2. This means that the red shift of the NH band induced by the solvent acidity is larger than that induced by the solvent basicity.

As for the LSER values (Table 3), the results exhibit a better correlation than the Swain equation. There are not only the specific interaction parameters (α and β), but also the non-specific interaction parameter (π*) for the LSER model. The negative π* coefficient informs that the red shift of ν(NH) is observed by non-specific solvent effects. The π* coefficients have the largest absolute values among the others. Therefore, the non-specific solvent effects are dominant in the interactions. The specific interaction parameters are also negative like $A_j$ and $B_j$ in the Swain equation. This also states the same influence as for the red shift of the NH bands by the solvent HBD acidity and HBA basicity. The α coefficient is larger than β. The NH stretching frequencies are more susceptible to the solvent HBD acidity than the HBA basicity. The LSER model used the experimental values is a powerful tool to investigate the solvent effects [ 7, 8, 31 ]. However, the poor correlations obtained by the LSER and Swain equations for the theoretical data approve that the PCM model neglects the specific solvent effects and reflects the non-specific interactions. It has not perfectly captured the solvent effects observed in the experiments either.

**Conclusions.** To explore the solvent effects on the NH stretching of 1-4pypp, a theoretical DFT research has been undertaken. The results can be useful for analyzing the structures involving piperazine. The important conclusions drawn in the current research are:

(i) The minimum energies of the optimized structures decrease with the solvent polarity.

(ii) From lower to higher dielectric, the dipole moments and bond lengths increase whereas the frequencies of the solvent-induced NH stretching vibrations decrease. Also, these frequencies decrease when approaching the more stable energy.

(iii) It is worth noting that the compounds have large dipole moments and this is an essential criterion for the drug-receptor interaction [ 24, 32 ].

(iv) For the theoretical solvent-induced ν(NH) frequencies, the KBM model shows a good correlation while the Swain, LSER and *AN* parameters have poor correlations. Further, as compared with the Swain equation, the LSER model presents a quantitatively accurate and physically meaningful explanation of solvent-induced stretching frequency shifts.

**Acknowledgments.** The author acknowledges the facilities from Ege University and would like to thank the editor and reviewers for their useful comments to improve the manuscript.

*REFERENCES*

1. *Kharb R., Bansal K., Sharma A.K.* // Der Pharma Chemica. – 2012. – **4**. – P. 2470 – 2488.
2. *Demerson C.A., Jirkovsky I.L.* // American Home Products Corp. – 1982. – US 4355031.
3. *Liu Y., Zhou E., Yu K., Zhu J., Zhang Y., Xie X., Li J., Jiang H.* // Molecules. – 2008. – **13**. – P. 2426 – 2441.

4. *Taniguchi N., Shirouchi Y.* // Nippon Shinyaku Co. – 2001. – WO 01/043746.
5. *Levinson N.M., Fried S.D., Boxer S.G.* // J. Phys. Chem. B. – 2012. – **116**. – P. 10470 – 10476.
6. *Chen Y., Morisawa Y., Futami Y., Czarnecki M.A., Wang H.S., Ozaki Y.* // J. Phys. Chem. A. – 2014. – **118**. – P. 2576 – 2583.
7. *Jovic B., Nikolic A., Petrovic S.* // J. Mol. Struct. – 2013. – **1044**. – P. 140 – 143.
8. *Ji X., Li Y., Zheng J., Liu Q.* // Mat. Chem. Phys. – 2011. – **130**. – P. 1151 – 1155.
9. *Vdovenko S.I., Gerus I.I., Kukhar V.P.* // Spectrochim. Acta A. – 2008. – **71**. – P. 779 – 785.
10. *Stolov A.A., Herrebout W.A., van der Veken B.J.* // J. Mol. Struct. – 1999. – **480** – **481**. – P. 499 – 503.
11. *Bruni P., Conti C., Galeazzi R., Giardina A., Giorgini E., Maurelli E., Tosi G.* // J. Mol. Struct. – 1999. – **480-481**. – P. 379 – 385.
12. *Cha J.N., Cheong B.S., Cho H.G.* // J. Mol. Struct. – 2001. – **570**. – P. 97 – 107.
13. *Sowula M., Misiaszek T., Bartkowiak W.* // Spectrochim. Acta A. – 2014. – **131**. – P. 678 – 685.
14. *Kirkwood J.G., Edwards R.T.* // J. Chem. Phys. – 1937. – **5**. – P. 14 – 22.
15. *Bauer E., Magat M.* // J. Physique Radium. – 1938. – **9**. – P. 319 – 330.
16. *Gutmann V., Resch G.* // The Donor-Acceptor Interactions. – New York: Plenum Press, 1978.
17. *Swain C.G., Swain M.S., Powell A.L., Alunni S.* // J. Am. Chem. Soc. – 1983. – **105**. – P. 502 – 513.
18. *Kamlet M.J., Abboud J.L.M., Abraham M.H., Taft R.W.* // J. Org. Chem. – 1983. – **48**. – P. 2877 – 2887.
19. *Tursun M., Keşan G., Parlak C., Şenyel M.* // Spectrochim. Acta A. – 2013. – **114**. – P. 668 – 680.
20. *Güneş E., Parlak C.* // Spectrochim. Acta A. – 2011. – **82**. – P. 504 – 512.
21. *Alver Ö., Parlak C.* // J. Theo. Comput. Chem. – 2010. – **9**. – P. 667 – 685.
22. *Alver Ö., Şenyel M.* // Chemical Papers. – 2010. – **64**. – P. 504 – 514.
23. *Mary Y.S., Panicker C.Y., Varghese H.T., Alsenoy C.V., Procházková M., Ševcík R., Pazdera P.* // Spectrochim. Acta A. – 2014. – **121**. – P. 436 – 444.
24. *Tursun M., Parlak C.* // Spectrochim. Acta A. – 2015. – **141**. – P. 58 – 63.
25. *Frisch M.J., Trucks G.W., Schlegel H.B. et al.* Gaussian 09, Revision A.1, Gaussian Inc., Wallingford, CT, 2009.
26. *Dennington R.D., Keith T.A., Millam J.M.* GaussView, Version 5.0.8, Gaussian Inc., Wallingford, CT, 2008.
27. *Miertus S., Scrocco E., Tomasi J.* // Chem. Phys. – 1981. – **55**. – P. 117 – 129.
28. *Merrick J.P., Moran D., Radom L.* // J. Phys. Chem. – 2007. – **111**. – P. 11683 – 11700.
29. *Marcus Y.* // Chem. Soc. Rev. – 1993. – **22**. – P. 409-416.
30. *Katritzky A.R., Fara D.C., Kuanar M., Hur E., Karelson M.* // J. Phys. Chem. A. – 2005. – **109**. – P. 10323 – 10341.
31. *Chen Y., Zhang H., Liu Q.* // Spectrochim. Acta A. – 2014. – **126**. – P. 122 – 128.
32. *Lien E.J., Guo Z.-R., Li R.-L., Su C.-T.* // J. Pharm. Sci. – 1982. – **71**. – P. 641 – 655.